

## Research paper

## Spatio-temporal salinity dynamics and yield response of rice in water-seeded rice fields

Mathias Marcos <sup>a,\*</sup>, Hussain Sharifi <sup>b</sup>, Stephen R. Grattan <sup>c</sup>, Bruce A. Linquist <sup>a</sup><sup>a</sup> Department of Plant Sciences, University of California – Davis, Davis, CA, 95616, USA<sup>b</sup> The Wonderful Company, Los Angeles, CA, 90064, USA<sup>c</sup> Department of Land, Air and Water Resources, University of California – Davis, Davis, CA, 95616, USA

## ARTICLE INFO

## Article history:

Received 23 December 2016

Received in revised form

23 September 2017

Accepted 26 September 2017

## Keywords:

Salinity dynamics

Rice

Yield threshold

Water quality modeling

Irrigation water quality

## ABSTRACT

The scarcity of high quality irrigation water is a global issue facing rice growers, forcing many to adopt water management systems that may result in increased salinity and yield reductions. While salt concentrations in field water have been shown to vary depending on water management, the distribution and build-up patterns of dissolved salts are unclear. This study was conducted to elucidate the within field spatial and temporal salinity dynamics in water-seeded rice cropping systems, and to assess current salinity thresholds for rice yield reduction. In this two-year study, water and soil salinity concentrations of eleven field sites were monitored weekly, with three sampling points being established in the top, middle and bottom basins of each field. There was a consistent spatio-temporal water salinity pattern among all fields: the maximum water salinity within a field occurred during week 2 to week 7 after planting, and was greatest farther from the irrigation inlet and where soil salinity was high. A model developed to predict water salinity within a field indicates that, averaged over an entire growing season, the position within a field contributed to 82% of the variation explained by the model, while preseason soil salinity contributed to 18%. Importantly, field water salinity was determined to be the most sensitive salinity metric for rice yield, as preseason soil salinity was a poor predictor of yield loss. The threshold field water salinity concentration was estimated at  $0.88 \text{ dS m}^{-1}$ , lower than the previous report of  $1.9 \text{ dS m}^{-1}$ . These results illustrate the ability to predict water salinity in a rice field with few parameters, while highlighting the importance of field water salinity as the main salinity metric for rice cropping systems.

© 2017 Elsevier B.V. All rights reserved.

## 1. Introduction

High quality water available for irrigated agriculture is currently scarce and is expected to become less available due to climate change and population growth (Hanak and Lund, 2012; Fraiture and Wigand, 2010; Mirchi et al., 2013; Schewe et al., 2014; Wallace 2000). This will result in increased use of marginal water and decreased drainage, thereby resulting in increased secondary salinization (Connor et al., 2012; Molden et al., 2010). Rice, a globally important staple crop, is the most salt-sensitive cereal (Grieve et al., 2012; Munns and Tester, 2008). Additionally, when grown under irrigation, rice requires two to three times more water input than other cereals (Bouman et al., 2007; Kijne 2006). The current and projected decline in the quantity and quality of water for rice pro-

duction, prompts the need to investigate salinity in rice cropping systems to avoid yield reductions.

In California, rice is the top agricultural water user based on application rate per hectare (USDA, 2013). Rice fields in California, which are typically divided into several hydrologically connected basins, are continuously flooded throughout the growing season, with irrigation water entering the topmost basin and cascading through to the bottommost basin. The primary water management system in California is a conventional flow-through system (hereafter referred to as “conventional-drainage”). Under conventional-drainage, tailwater discharges to a drainage ditch for much of the growing season; the exception being during water holding periods after pesticide applications, whereby tailwater drainage is temporary halted to allow for pesticide degradation in the field (Hill et al., 1991). Under conventional-drainage, the amount of tailwater drainage can be as high as  $7.6 \text{ ML ha}^{-1}$  (Hill et al., 2006) and 39% of the total water applied to a field (Linquist et al., 2015). Tailwater drainage helps remove salts that accumulate in the field water (Scardaci et al., 2002), thereby preventing

\* Corresponding author at: Department of Plant Sciences, University of California – Davis, Davis, CA, 95616, USA.

E-mail address: [mmarcos@ucdavis.edu](mailto:mmarcos@ucdavis.edu) (M. Marcos).

the long term accumulation of salt in the soil (Lekakis et al., 2015). Recent drought conditions in California have reduced the water available for rice production (Howitt et al., 2015), forcing many growers to reduce the amount of water applied to a field. A common method to reduce the water applied to a field is to eliminate the tailwater drainage (hereafter referred to as “zero-drainage”). While zero-drainage can greatly reduce the total water applied to a field, it is likely to increase the salinity concentration, particularly in bottom basins. Nevertheless, the projected future of decreased water available for rice production in California (Hill et al., 2006) will likely increase the practice of zero-drainage. This, along with an increased reliance on groundwater for irrigation, which has a higher salt concentration than surface water (Grattan 2002), may lead to high salinity in rice fields and reductions in yield.

Crop yield response to salinity is most often displayed using a piecewise linear model (Ayers and Westcot 1985; Maas and Grattan 1999; Maas and Hoffman 1977), where the first segment is a tolerance plateau with a slope of zero, and the second segment is a concentration dependent line with a negative slope (Supplementary Fig. 1). The threshold salinity concentration, the concentration beyond which crop yields decline, is of utmost concern to both growers and regulators. In flooded rice systems, a confounding factor is the need to account for both field water salinity (i.e. salinity of the ponded water) and soil salinity. Traditionally, field water and soil salinity thresholds for rice have been developed from studies with limited observations over a wide salinity range, resulting in large distances between salinity treatments and a large uncertainty in threshold estimates (Grieve et al., 2012). Additionally, salinity threshold studies occur under steady-state conditions, whereby salinity stress is kept constant throughout the growing season (Maas and Grattan 1999). Conversely, field water and soil salinity in commercial rice fields lack temporal uniformity (Scardaci et al., 1996; Scardaci et al., 2002), and the range of observed salinity concentrations is narrower and lower than in salinity threshold studies. The lack of relatedness between field and study conditions, and the uncertainty of threshold estimates, has led some to question the applicability of current thresholds (Kijne 2006; Shalhevett 1994), especially in rice, as yield loss has been reported below the threshold value (Simmonds et al., 2013). These discrepancies have increased the focus on developing thresholds under realistic field conditions (Kijne, 2006), thereby increasing the applicability of threshold estimates.

Elucidating the spatial and temporal salinity dynamics is vital to ameliorate salinity stress in rice fields, especially since rice is more sensitive to salinity from tillering to flowering (Castillo et al., 2007; Heenan et al., 1988; Fraga et al., 2010; Pearson and Bernstein 1959; Zeng et al., 2001). Additionally, there have been reports of decreased stand establishment in commercial rice fields due to high salinity early in the season (Scardaci et al., 2002; Shannon et al., 1998). Previous studies in commercial fields under conventional-drainage, have found that water salinity increased in bottom basins of fields (Scardaci et al., 2002 & Simmonds et al., 2013), likely due to evapo-concentration. Simmonds et al. (2013) also found water salinity to be higher in areas of the field away from the primary water flow path (i.e. low flow areas). Results from Simmonds et al. (2013) and Scardaci et al. (2002), suggest that location in a field, relative to the irrigation inlet and primary water flow path, largely determines the field water salinity concentration; though, it is unclear how applicable these results are in fields under zero-drainage. A complete understanding of the spatio-temporal salinity dynamics in rice fields, however, is essential to being able to properly manage salinity in rice fields. Therefore, the objectives of this study were to: 1) reassess salinity thresholds using commercial rice fields, 2) quantify spatial and temporal variation of water and soil

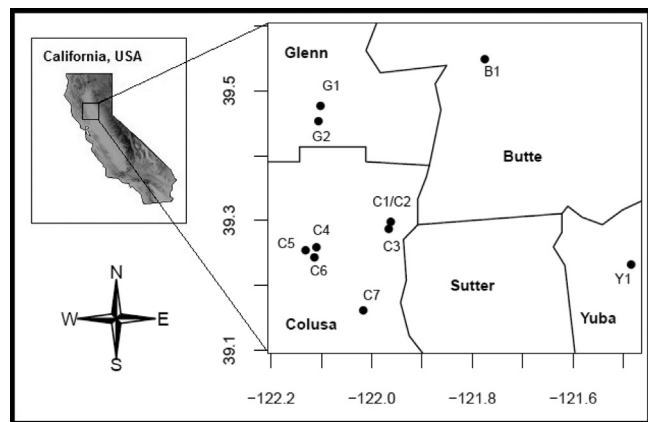


**Fig. 1.** A map illustrating the location of field sites for the study. Field names refer to the first letter of the counties they are in.

salinity in commercial rice fields and 3) develop a model to predict water salinity in fields under zero-drainage.

## 2. Materials and methods

### 2.1. Study area and site descriptions

This experiment was carried out in commercial rice fields throughout the Upper Sacramento Valley of California (Fig. 1) during the 2014 and 2015 rice growing seasons. Eleven field sites with zero tailwater drainage or conventional tailwater drainage, and a wide range of soil salinity, were chosen for this study. There were seven field sites in Colusa county (C1, C2, C3, C4, C5, C6, and C7), two in Glenn county, (G1 and G2), one in Butte county, (B1), and one in Yuba county, (Y1). This region has a Mediterranean climate, characterized by warm, dry conditions during the rice growing season. The mean air temperature during the 2014 and 2015 growing seasons was 22.7 °C, while the mean precipitation during the growing seasons was 15 mm (CIMIS, 2016). All field sites have fine-textured soils with minimal slope, which is typical for rice fields in the region. Soil taxonomic classifications, soil characteristics, irrigation practices and variety sown are shown in Table 1. Field-specific pesticide regimens were employed to combat weeds and insect pests.

### 2.2. Experimental design

Each field site contained 9 plots (2 m × 2 m) that were split between the top (A), middle (B) and bottom(C) basins (Fig. 2). Within each basin, three sampling plots were established and numbered (1, 2, 3) based on their proximity to the primary water flow path (plot 1 being closest and plot 3 being farthest from the primary water flow path). For basins B and C, if water flowed down from both sides of the field, then plot 3 was in the middle of the basin (as shown in Fig. 2). If water flowed from only one side of the field, then plots in the B and C basins were spaced similar to the A basin. All plots were established 15 m in from the edge of the field to avoid border effects. Fig. 2 is a representation of the plot design within a field; however, field sites varied in dimension and number of basins. The position of each plot was determined in each field, with the position within a field being considered as the combination of the longitudinal distance down the field and the lateral distance across a basin (as shown in Fig. 2).

### 2.3. Sampling and measurements

After spring land preparation, but before fertilizer application and flooding, soil samples were taken from each plot at a depth of

**Table 1**  
Overview of site soil characteristics and water management.

Field	Soil Taxonomic Classification	Field Size (ha)	Number of Basins	Soil Texture			SOC (%)	pH	Field EC <sub>e</sub> (dS m <sup>-1</sup> )	SAR	Tailwater Drainage	Cultivar
				Sand (%)	Silt (%)	Clay (%)						
C1	Fine, smectitic, thermic Sodic Endaquerts	44	7	10	57	33	2.15	6.26	1.13	4.60	Zero	M-206
C2	"	44	7	10	57	33	2.26	6.35	0.99	4.27	Zero	M-206
C3	"	64	6	8	56	36	2.52	6.05	0.85	3.18	Zero	M-206
C4	"	32	3	12	28	60	2.04	7.46	5.88	8.31	Conventional	M-206
C5	"	17	2	12	27	61	2.22	6.56	5.69	7.93	Conventional	M-202
C6	"	36	3	12	27	61	1.54	7.09	6.25	8.37	Zero	M-206
C7	"	21	6	21	45	34	1.79	6.93	4.49	8.43	Conventional	Calhikari-202
G1	Fine, thermic Typic Calciaquolls	45	9	20	40	40	2.20	5.76	0.50	1.17	Zero	M-206
G2	"	31	4	13	44	43	2.10	5.76	0.59	1.72	Zero	M-208
B1	Fine, smectitic, thermic Xeric Epiaquerts and Dur aquerts	24	3	31	23	46	1.90	4.94	0.33	0.91	Zero	M-105
	Fine, mixed thermic Abruptic Durixeralfs	30	3	43	37	20	1.19	4.59	0.29	0.88	Zero	M-206
Y1												

" Same as above; SOC: soil organic carbon; SAR: sodium adsorption ratio; EC<sub>e</sub>: preseason soil saturated paste salinity.

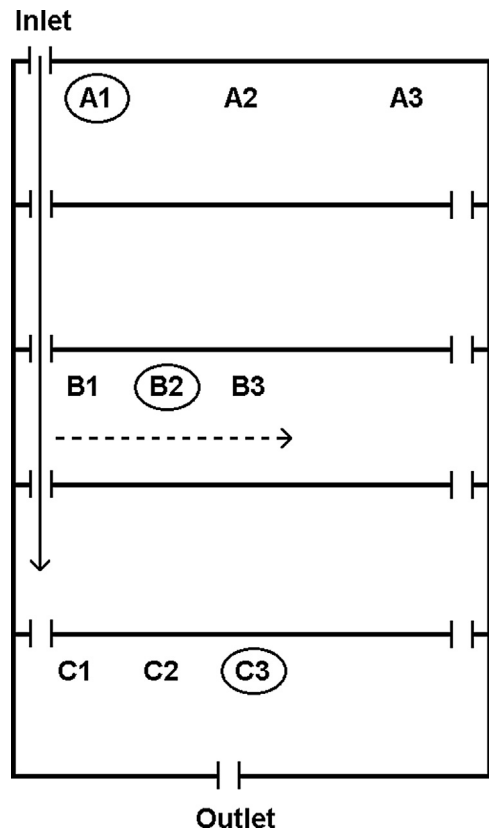


**Fig. 2.** A map illustrating the experimental set up within a field. The solid line and arrow on the left represents the longitudinal distance down the field, while the dashed lines and arrows represent the lateral distance across a basin. Plots are represented by a letter & number combination. A plots location in a field is a combination of the longitudinal and lateral distance from the irrigation inlet. Water salinity measurements were collected at all plots. Soil solution salinity measurements were collected at circled plots.

0–15 cm. Soils were air dried, then ground to pass through a 2-mm sieve. For each field site, equally weighted portions of the soil samples were mixed to generate a composite field sample, from which, general field soil property data were determined (Table 1). Soil pH, soil texture, sodium adsorption ratio, and soil organic carbon were determined from the composite field samples using standard methods described in the Soil Survey Laboratory Methods Manual (Burt, 2014).

Four types of salinity measurements, all based on electrical conductivity (EC), were made in this study using a calibrated Oakton CON 450 or an Oakton CON 400 (Vernon, IL, USA) standardized to 25 °C. Throughout the growing season, weekly water salinity measurements were made at the irrigation inlet (EC<sub>iw</sub>), and at all plot locations (EC<sub>fw</sub>). To obtain the measurements, the EC probe was carefully lowered into the water and kept submerged until a stable reading was reached. Soil samples taken from each plot prior to flooding were used to determine the preseason soil salinity (EC<sub>e</sub>) using the saturated paste technique (Burt, 2014). Additionally, weekly in-season soil solution salinity (EC<sub>ss</sub>) measurements were made, at the same time as EC<sub>fw</sub> measurements, at A1, B2, and C3 plots (Fig. 2). In order to obtain EC<sub>ss</sub> measurements, before flooding, soil pore-water samplers (Rhizon MOM 10 cm, Rhizosphere Research Products, Wageningen, The Netherlands) were installed 10 cm below the soil surface. Before obtaining EC<sub>ss</sub> measurements, the hose of the pore-water sampler was purged by extracting the first 10 mL of solution into evacuated vials. Soil solution was then extracted into evacuated 40 mL vials, and EC<sub>ss</sub> was measured *in situ*.

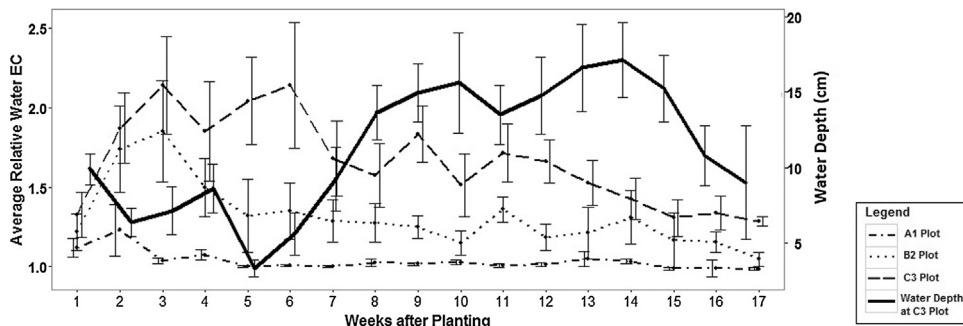


**Fig. 3.** Temporal pattern of average relative water EC (field water salinity relative to irrigation water salinity) at A1, B2, and C3 plots. Average water depth in the C3 plot is shown on the right axis. Water depth in other basins has a similar pattern (data not shown). Error bars represent standard error.

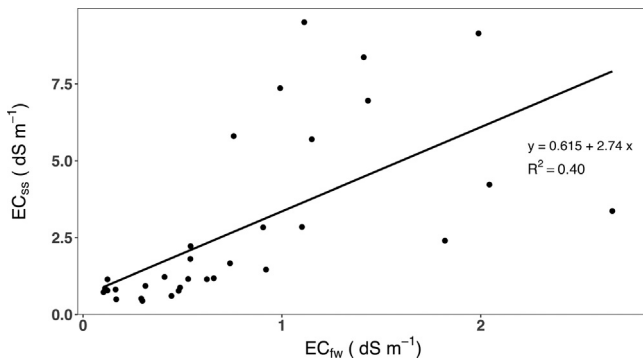


**Fig. 4.** The relationship between season-average field water salinity ( $EC_{fw}$ ) and season-average soil solution salinity( $EC_{ss}$ ).

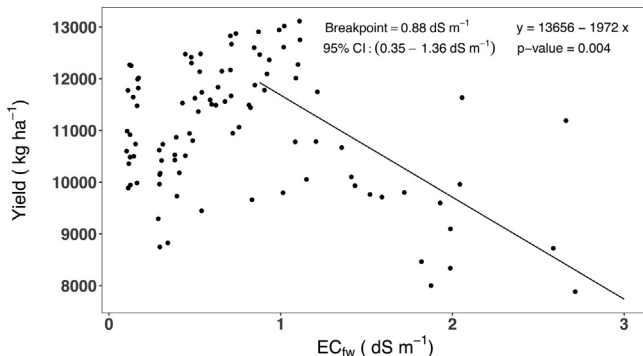


**Fig. 5.** The relationship between yield ( $kg ha^{-1}$ ) and season-average field water salinity ( $EC_{fw}$ ). Yield is negatively correlated with field water EC above  $0.88 dS m^{-1}$ . This figure only includes the significant fixed effects.

Field water depth measurements were taken at the same locations and at the same time as the  $EC_{ss}$  measurements.

Upon physiological maturity (grain moisture content below 28%) yield was quantified at all plot locations. A 1-m<sup>2</sup> undisturbed representative area within each plot was hand harvested and then a sub-sample was oven-dried at 70 °C until a constant weight was achieved. Samples were then processed to determine total above-ground biomass and grain yield. Grain yield was corrected to 14% moisture content.

#### 2.4. Data analysis

R statistical software (R Core Team, 2015) was used for data analysis and visualization. The following packages were used for data visualization: 'ggplot2' (Wickham and Chang 2016), 'gttable' (Wickham, 2016), 'maps' (Becker et al., 2016), 'maptools' (Bivand and Lewin-Koh 2016), and 'raster' (Hijmans, 2015).

For comparisons of soil and water salinity between the top (A1) and bottom (C3) of a field, a one sample *t*-test was performed. Results are reported as a percent increase from the top to the bottom basin.

Salinity yield threshold analysis was conducted by determining the convergence point of two linear regression lines seeking to minimize overall deviance. To account for potential difference in yield at the field scale, a mixed-effects modeling approach was employed using the 'lme4' (Bates et al., 2016) package. In this approach, field site was a random effect and was allowed to have its own intercept (i.e. yield potential).

While a water salinity threshold was determined, this study was unable to identify a threshold for soil salinity. Nevertheless, the potential effect of soil salinity on yield was assessed using the  $EC_e$  of plot locations above the water salinity threshold. The relative importance of soil salinity on yield was evaluated by comparing three mixed-effects models (1–3) developed using the 'lme4' (Bates et al., 2016) package:

$$Y_{ij} = a_j + B_1 * x_{ij} + e_{ij} \quad (1)$$

$$Y_{ij} = a_j + B_2 * z_{ij} + e_{ij} \quad (2)$$

$$Y_{ij} = a_j + B_1 * x_{ij} + B_2 * z_{ij} + e_{ij} \quad (3)$$

where  $Y_{ij}$  is the yield at plot  $i$  in field  $j$ ,  $a_j$  is the intercept for field  $j$ ,  $x_{ij}$  is the water salinity at plot  $i$  in field  $j$ ,  $z_{ij}$  is the soil salinity at plot  $i$  in field  $j$ ,  $B_1$  is the water salinity coefficient,  $B_2$  is the soil salinity coefficient, and  $e_{ij}$  is the error term for plot  $i$  in field  $j$ . The relative importance of field water and soil salinity to yield loss was assessed by comparing the Akaike's Information Criterion adjusted for a small sample size ( $AIC_c$ ), marginal  $R^2$  values of the models, and the significance of the model coefficients. The 'MuMIn' (Bartoň, 2016) package was used to determine  $AIC_c$  values of the models, with the lowest  $AIC_c$  value indicating the best model (Burnham and Anderson 2002). The 'MuMIn' (Bartoň, 2016) package was also used to determine marginal  $R^2$  values for the mixed-effects models; the method used follows the procedure described by Nakagawa and Schielzeth (2013), where marginal  $R^2$  is the proportion of variation explained by the fixed factors. The 'lmerTest' package (Kuznetsova et al., 2016) was used to determine  $p$  values for the mixed-effects models.

As field salinity concentrations varied based on field location and source of irrigation water, comparisons of field water salinity among field sites were made relative to the irrigation water salinity. During the season, the C2 site began receiving water from multiple irrigation inlets and could not be used for this analysis. Using fields under zero-drainage, a predictive model for season-average relative field water salinity was developed based on *a priori* knowledge

of potential parameters that may influence water salinity: position within a field and soil salinity. One superior model emerged (4):

$$S_{ij} = a + B_3 * w_{ij} + B_4 * u_{ij} + B_5 * q_{ij} + e_{ij} \quad (4)$$

where  $S_{ij}$  is the salinity of plot  $i$  in field  $j$  relative to the salinity of the irrigation water into field  $j$ ,  $a$  is the intercept,  $w_{ij}$  is the longitudinal distance down the field from the irrigation inlet for plot  $i$  in field  $j$ ,  $u_{ij}$  is the lateral distance across a basin from the irrigation inlet or basin inlet for plot  $i$  in field  $j$ ,  $q_{ij}$  is the preseason soil salinity of plot  $i$  in field  $j$ ,  $e_{ij}$  is the error term for plot  $i$  in field  $j$ , and  $B_3$ ,  $B_4$ , and  $B_5$  are model coefficients. Parameters from this season-average model were used to develop early and late-season models to assess variable contributions throughout the growing season. Early-season is defined as week 1 to week 7 after planting, while late-season is defined as week 8 to week 15 after planting. The 'relaimpo' package (Groemping and Matthias, 2013) was used to assess variable contributions to the models; this was done by  $R^2$  partitioning, as done by Lindeman et al. (1980). Model performance was assessed through leave-one-field-out (LOFO) cross-validation, as employed in other field-based agricultural studies (Pike et al., 2009; Scudiero et al., 2015; Stevens et al., 2012), using the 'caret' package (Kuhn 2016). In this LOFO cross-validation approach, a model is developed using data from six of the seven usable fields under zero-drainage. The model is then used to generate predictions for the seventh field. This procedure is repeated seven times so that each field is left out once. Finally, after model validation, data from all seven zero-drainage fields were used to develop the final models.

### 3. Results

#### 3.1. Site salinity conditions

Field average preseason soil salinity ( $EC_e$ ) ranged from 0.29 to  $6.25 \text{ dS m}^{-1}$  (Table 1). In general, fields with lower preseason soil salinity were under zero-drainage, while fields with higher pre-season soil salinity, were under conventional-drainage, with the exception of C6, which was under zero-drainage. The irrigation water salinity ( $EC_{iw}$ ) of fields under zero-drainage ranged from 0.08 to  $1.38 \text{ dS m}^{-1}$ , while  $EC_{iw}$  of fields under conventional-drainage ranged from 0.39 to  $2.92 \text{ dS m}^{-1}$  (Table 2). Fields supplied with groundwater had a higher  $EC_{iw}$  than fields supplied solely with surface water. Additionally, the  $EC_{iw}$  of fields supplied with surface water, which is under irrigation district control, varied largely based on the proportion of recycled water allowed by the irrigation district.

#### 3.2. Spatial and temporal field water and soil solution salinity dynamics

Fields differed in size and shape, leading to variation in field water salinity ( $EC_{fw}$ ) and soil solution salinity ( $EC_{ss}$ ) build-up throughout the field; however, on average, season-average  $EC_{fw}$  and  $EC_{ss}$  were 79% and 130% higher, respectively, in bottom basins compared to the top basins (Table 3). Within a field, the maximum observed  $EC_{fw}$  tended to occur in the bottom basin between week 2 and week 7 after planting, and ranged from  $0.36$  to  $6.06 \text{ dS m}^{-1}$  (Table 2). Spikes in  $EC_{fw}$  early in the season tended to coincide with low field water depth (Fig. 3). There was no consistent temporal  $EC_{ss}$  trend among fields (data not shown). Additionally, while there was a positive correlation ( $R^2=0.40$ ) between season-average  $EC_{fw}$  and season-average  $EC_{ss}$  (Fig. 4), there is poor correlation when  $EC_{ss} > 3 \text{ dS m}^{-1}$ .

**Table 2**  
Overview of irrigation water salinity ( $EC_{iw}$ ), field water salinity ( $EC_{fw}$ ), and soil solution salinity ( $EC_{ss}$ ) concentrations observed in the study.

Irrigation Water EC	Field Water EC	Average $EC_{fw}$ ( $\text{dS m}^{-1}$ )	Range ( $\text{dS m}^{-1}$ )	Min $EC_{fw}$ ( $\text{dS m}^{-1}$ )	Max $EC_{fw}$ ( $\text{dS m}^{-1}$ )	Plot/Week	Average $EC_{ss}$ ( $\text{dS m}^{-1}$ )	Min $EC_{ss}$ ( $\text{dS m}^{-1}$ )	Max $EC_{ss}$ ( $\text{dS m}^{-1}$ )	Plot/Week
C1 Surface	0.47	0.31–0.64	0.62	0.33[A1/W10	1.64[C2/W4	1.65	0.43[A1/W2	3.69[C3/W16		
C2 Ground & Surface	0.45	0.29–0.74	0.76	0.25[A1/W3	2.10[C2/W5	1.79	0.43[A1/W8	3.51[C3/W6		
C3 Surface	0.62	0.31–0.75	0.75	0.33[A1/W9	2.45[B3/W3	1.28	0.73[A1/W1	2.30[C3/W4		
C4 <sup>a</sup> Ground & Surface	0.11	0.42–1.70	1.46	0.49[C1/W2	6.06[C3/W6	7.55	4.55[A1/W14	11.35[C2/W2		
C5 <sup>a</sup> Surface	0.54	0.39–0.66	0.82	0.43[A1/W1	4.19[C3/W7	5.70	1.69[A1/W7	12.28[C2/W1		
C6 Surface	0.71	0.41–1.38	0.99	0.40[A1/W3	2.08[A3/W2	7.81	4.35[A1/W16	11.95[C2/W5		
C7 <sup>a</sup> Ground	1.81	1.12–2.92	2.10	1.11[A1/W14	4.44[C3/W7	3.49	1.89[A1/W15	5.35[C3/W7		
G1 Surface	0.30	0.24–0.43	0.37	0.19[A3/W5	0.72[C3/W3	0.84	0.31[A1/W13	1.56[B2/W3		
G2 Surface	0.28	0.18–0.40	0.35	0.17[A3/W11	0.80[C3/W13	1.06	0.32[A1/W4	2.81[C3/W13		
B1 Surface	0.11	0.08–0.24	0.15	0.08[C3/W7	0.36[C1/W10	0.75	0.11[B2/W7	1.36[C3/W16		
Y1 Surface	0.09	0.08–0.13	0.12	0.06[B1/W7	0.06[C1/W4	0.90	0.08[A1/W6	2.17[C3/W2		

<sup>a</sup> field with conventional tailwater drainage;  $EC_{iw}$ : irrigation water salinity;  $EC_{fw}$ : field water salinity;  $EC_{ss}$ : soil solution salinity.

**Table 3**

Relative increases of soil or field water salinity from the top of field (A1 plot) to bottom of the field (C3 plot), with the 95% confidence interval in parentheses.

Relative Increase from top (A1) to bottom (C3) (%)	
EC <sub>fw</sub>	78.8 *** (46.2–111.5)
EC <sub>ss</sub>	130.0 ** (42.3–217.6)
EC <sub>e</sub>	53.4 ** (17.1–89.8)

EC<sub>fw</sub>: field water salinity. EC<sub>ss</sub>: soil solution salinity.

EC<sub>e</sub>: preseason soil saturated paste salinity.

\*, \*\*, \*\*\*, correspond to the 0.05, 0.01, and 0.001 significance level.

**Table 4**

Parameter estimates for mixed-effects models for yield loss due to salinity. Field site was a random effect. Only field water EC values greater than the threshold (0.88 dS m<sup>-1</sup>) were used for these models.

Mixed Effects Model	Fixed Effects	Estimate	95% Confidence Interval
Field water EC Model			
	Intercept	13656.0 ***	12278–14903
	EC <sub>fw</sub>	−1971.8 **	−2756 – −1151
	Marginal R <sup>2</sup>	0.46	
	AIC <sub>c</sub>	533.97	
Soil EC Model			
	Intercept	12475.2 ***	10844 – 14088
	EC <sub>e</sub>	−334.6	−654–2
	Marginal R <sup>2</sup>	0.16	
	AIC <sub>c</sub>	537.5	
Field water + Soil EC Model			
	Intercept	14349.4 ***	12897 – 15827
	EC <sub>fw</sub>	−1941.5 ***	−2662 – −1226
	EC <sub>e</sub>	−154.5	−375 – 47
	Marginal R <sup>2</sup>	0.50	
	AIC <sub>c</sub>	534.97	

\*\*\*, \*\*\*, correspond to the 0.05, 0.01, and 0.001 significance level.

### 3.3. Yield results

Using a mixed-effects modeling approach, a significant negative correlation was observed between yield and field water salinity above 0.88 dS m<sup>-1</sup>, with a 95% confidence interval of 0.35–1.36 dS m<sup>-1</sup> (Fig. 5). In contrast, the same approach did not result in a significant breakpoint for EC<sub>ss</sub> and EC<sub>e</sub> (data not shown), potentially due to the nature of the data. There was a gap in EC<sub>e</sub> values between 1.88 and 3.88 dS m<sup>-1</sup> (Supplementary Fig. 2), and only three EC<sub>ss</sub> data points per field. Therefore, the effect that soil salinity may have on yield loss was further assessed by comparing models that included and excluded EC<sub>e</sub> and EC<sub>fw</sub> terms (Table 4), which helped to determine the importance of the two variables to yield loss. The yield model with solely EC<sub>fw</sub> resulted in a significant regression coefficient of −1971.8 kg ha<sup>-1</sup> per dS m<sup>-1</sup> and had a marginal R<sup>2</sup> of 0.46 (Table 4). The yield model with solely EC<sub>e</sub> did not produce a significant regression coefficient, and had a marginal R<sup>2</sup> of 0.16. The yield model with both EC<sub>fw</sub> and EC<sub>e</sub> produced a significant regression coefficient for EC<sub>fw</sub> but not for EC<sub>e</sub>, while the marginal R<sup>2</sup> was 0.50. Additionally, the model with only EC<sub>fw</sub> had a lower AIC<sub>c</sub> value than the models with only EC<sub>e</sub> or with both EC<sub>fw</sub> and EC<sub>e</sub>.

### 3.4. Modeling field water salinity

A model was developed that predicts season-average EC<sub>fw</sub> in zero-drainage fields based on incoming irrigation water salinity, the lateral and longitudinal distance from the inlet, and preseason soil salinity, with R<sup>2</sup> of 0.69 when evaluated against all data and R<sup>2</sup> of 0.60 for the LOFO cross-validation predictions (Table 5). For the season-average water salinity model, lateral and longitudinal distance together contributed to 82% of the explained variance in

**Table 5**

Model accuracy parameters (R<sup>2</sup> and Root Mean Squared Error (RMSE)) between predictions from Eq. (4) and ground-truth values. For Observed, the entire dataset was fit to Eq. (4). For Validation, the leave-one-field-out cross-validations were fit to Eq. (4). The season average model includes measurements from week 1 to week 15 after planting. The early season model includes measurements from week 1 to week 7 after planting. The late season model includes measurements from week 8 to week 15 after planting.

Model	Observed		Validation	
	R <sup>2</sup>	RMSE	R <sup>2</sup>	RMSE
Season Average	0.69	0.149	0.60	0.171
Early Season	0.76	0.194	0.68	0.227
Late Season	0.57	0.149	0.19	0.239

the model, while preseason soil salinity contributed 18% (Table 6). Model results for the early-season (week 1 to week 7 after planting) indicate that preseason soil salinity had a larger effect and contributed to 49% of the explained variance in the model, while lateral and longitudinal distance contributed to the remaining 51% (Table 6). In contrast, preseason soil salinity did not have a significant effect in the late-season (week 8 to week 15 after planting) (Table 6). The early-season model also performed better than the late-season model, as the validation R<sup>2</sup> for the early-season model was 0.68, compared to 0.19 for the late-season model (Table 5). Additionally, while fields with conventional-drainage were not included in the development of the models, in the early-season model, observed relative water salinity of fields with conventional-drainage was always lower than the predicted value (Fig. 6).

## 4. Discussion

### 4.1. Field water EC is the most sensitive salinity metric for rice yield

Soil and water salinity are both commonly used to determine whether rice yield may be adversely affected by salinity (Ayers and Westcot 1985; Maas and Grattan 1999). In this study, there were two soil salinity metrics, preseason soil salinity (EC<sub>e</sub>), which came from samples collected at each plot from 0 to 15 cm below the soil surface prior to flooding, and soil solution salinity (EC<sub>ss</sub>), which were weekly pore-water measurements at 10 cm below the soil surface. Though there was a good correlation ( $R^2 = 0.89$ ) between season-average EC<sub>ss</sub> and preseason EC<sub>e</sub> (Supplementary Fig. 3), the two soil salinity metrics were employed for different analyses. To observe the relationship between soil and field water salinity, EC<sub>ss</sub> was used, as there were measurements for this metric at the same time and location as EC<sub>fw</sub>. To study the relationship with yield, EC<sub>e</sub> was used, as there were EC<sub>e</sub> measurements at all plot locations. Additionally, growers are more likely to gather soil samples before the season, when the field is dry, and this is therefore a more appropriate metric for yield.

In this study, a positive correlation ( $R^2 = 0.40$ ) was observed between season-average EC<sub>fw</sub> and season-average EC<sub>ss</sub> (Fig. 4). Similarly, Dickey and Nuss (2002) and Scardaci et al. (2002), found within-season correlations of soil and water salinity, with R<sup>2</sup> values ranging from 0.52 to 0.70. Grattan et al. (2002) found season-average EC<sub>fw</sub> and postseason EC<sub>e</sub> to correlate with  $R^2 = 0.88$ . High correlations between soil and field water salinity led Grattan et al. (2002) and Dickey and Nuss (2002) to effectively equate soil salinity (averaged from 0 to 15 cm below the soil surface), with field water salinity. The poor correlation between EC<sub>fw</sub> and EC<sub>ss</sub> observed at EC<sub>ss</sub> values  $>3$  dS m<sup>-1</sup> (Fig. 4) questions this approach. At lower soil salinity concentrations there seems to be good correlation between soil and field water salinity but at higher soil salinity concentrations there is no clear relationship. The poor correlation at higher

**Table 6**

Model coefficients and variable contributions to the models to predict relative water EC (field water salinity relative to the irrigation water salinity) in zero-drainage fields. These models were developed using data from all fields. The variable contributions to the explained variation are normalized to sum 100%. The season average model includes measurements from week 1 to week 15 after planting. The early season model includes measurements from week 1 to week 7 after planting. The late season model includes measurements from week 8 to week 15 after planting. The 95% confidence intervals of the estimates are in parentheses below each estimate.

Model	Model Coefficients				Variable Contribution to explained R <sup>2</sup> (%)		
	Intercept	Longitudinal Distance	Lateral Distance	Preseason EC <sub>e</sub>	Longitudinal Distance	Lateral Distance	Preseason EC <sub>e</sub>
Season Average	9.293e-01 *** (8.31e-01–1.028)	5.057e-04 *** (3.998e-04–6.116e-04)	9.994e-04 *** (6.20e-04–1.379e-03)	4.887e-02 *** (2.884e-02–6.890e-02)	68.9	13.4	17.7
Early Season	8.668e-01 *** (7.380e-01–9.956e-01)	6.196e-04 *** (4.808e-04–7.585e-04)	1.051e-03 *** (5.492e-04–1.553e-03)	1.225e-01 *** (9.627e-02–1.487e-01)	46.6	4.4	49.0
Late Season	9.796e-01 *** (8.809e-01–1.078)	4.270e-04 *** (3.204e-04–5.337e-04)	7.799e-04 *** (3.975e-04–1.162e-03)	-8.691e-03 (-2.884e-02–1.146e-02)	79.1	19.2	1.7

\*, \*\*, \*\*\*, correspond to the 0.05, 0.01, and 0.001 significance level.

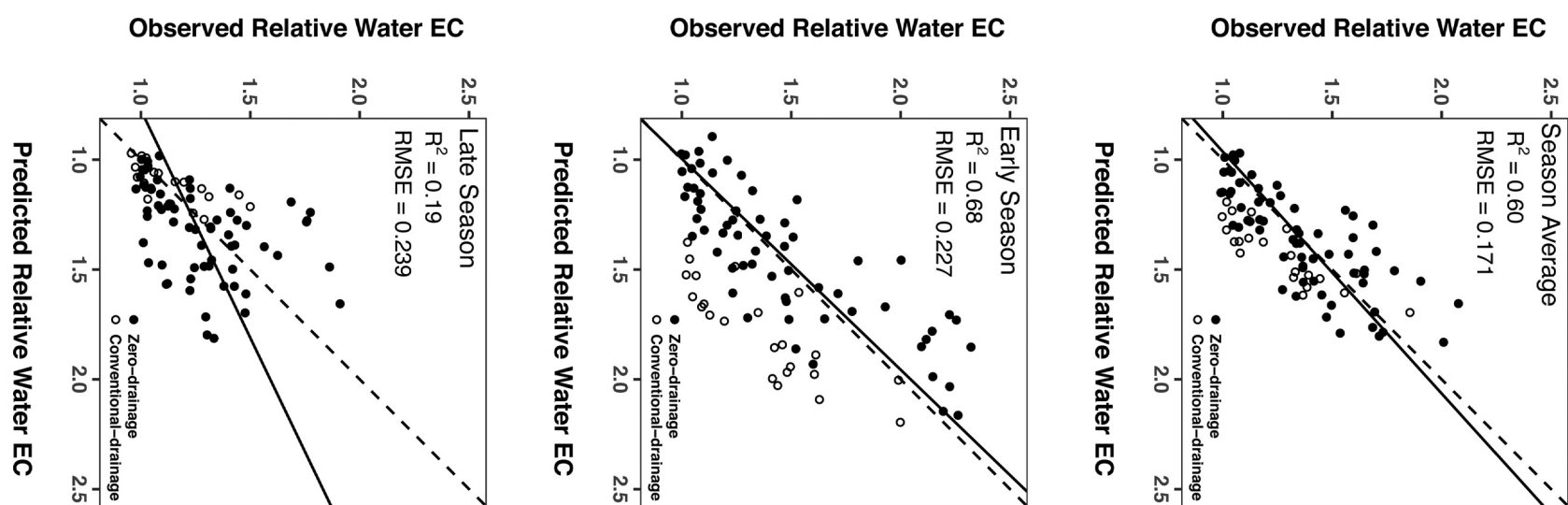


**Fig. 6.** Relationships between observed relative water EC (field water salinity relative to irrigation water salinity) and leave-one-field-out validation predictions using Eq. 4 for season-average, early-season, and late-season models in fields under zero-drainage (filled dots). Fields under conventional-drainage were not included in the development of the models; however, the relationship between observed relative water EC and predictions using the final model are shown (unfilled dots).

soil salinity necessitates differentiation between soil salinity and field water salinity in flooded rice cropping systems.

Field water salinity correlated better with yield, and produced a better model based on AIC<sub>c</sub> values, than did preseason soil salinity (Table 4). Furthermore, adding preseason soil salinity to the model with field water salinity did not produce a significant regression coefficient for soil salinity, worsened the model based on AIC<sub>c</sub> values, and did not greatly improve the models predictive capacity. These results, along with high yields observed under high EC<sub>e</sub> (Supplementary Fig. 2) and high EC<sub>ss</sub> (Supplementary Fig. 4), suggest that EC<sub>fw</sub> is the most sensitive index when seeking to predict salinity induced yield loss.

Rice yield responding primarily to water salinity stress may be explained by the morphology of rice roots. Under flooded culture, rice plants develop many surface roots (Morita and Yamazaki 1993), and the rooting depth is partially controlled by environmental conditions (Yoshida 1981). Previous studies have shown that under heterogeneous salinity conditions, roots take up water from the least saline areas (Bazihizina et al., 2012; Homaei and Schmidhalter 2008). It is therefore likely that in fields where soil salinity is much higher than water salinity, rice roots preferentially developed and absorbed water from the surface, and thereby only exhibited a response to water salinity stress.

#### 4.2. Threshold concentration of field water salinity is lower than previously reported

The effect field water salinity will have on rice yield is a combination of the salt concentration, the length of exposure to the stress, and the plant susceptibility at that growth stage (Läuchli and Grattan 2007). While it is known that rice is very sensitive to salinity during tillering (Heenan et al., 1988; Pearson and Bernstein 1959; Zeng et al., 2001) and during reproduction (Castillo et al., 2007; Heenan et al., 1988; Fraga et al., 2010), it is not clear which growth stage is most sensitive to salinity nor the relative contribution that salinity stress would have to yield loss if salinity stress occurred during multiple growth stages. Additionally, reductions in stand establishment were not observed in this study. Therefore, water salinity concentrations used for the yield threshold analysis were a season-average EC<sub>fw</sub> developed from weekly field water salinity measurements averaged over the duration of the growing season in which the field was flooded. This approach is similar to that taken by others that have contributed to threshold estimates in rice (Ehrler 1960; Grattan et al., 2002; Narale et al., 1969; Pearson 1959; Venkateswarlu et al., 1972). While this study was able to develop a yield threshold for field water salinity, the narrow range of season-average field water salinity observed ( $0.10\text{--}2.72 \text{ dS m}^{-1}$ ), prevents characterization of crop yield response to very high field water salinity.

The season-average EC<sub>fw</sub> yield threshold was estimated to be  $0.88 \text{ dS m}^{-1}$  (Fig. 5). This threshold is well below the previous report of  $1.9 \text{ dS m}^{-1}$  (Grattan et al., 2002) and this may be due to the different conditions under which values were obtained. Grattan et al. (2002) conducted their study under steady-state conditions, whereby salinity concentrations remained constant from seeding to maturity. In contrast, in this study, field water salinity varied during the growing season (Table 2; Fig. 3), with rice plants experiencing spikes in salinity during tillering, a very salt-sensitive growth stage (Heenan et al., 1988; Fraga et al., 2010; Pearson and Bernstein 1959; Zeng et al., 2001). This resulted in a lower threshold

The early-season model includes measurements from week 1 to week 7 after planting. The late-season model includes measurements from week 8 to week 15 after planting. The season-average model includes measurements from week 1 to week 15 after planting. R<sup>2</sup> and Root Mean Squared Error (RMSE) are reported in the figure. The dashed line is a 1:1 line, while the solid line is the line of best fit.

estimate, as the season-average salinity concentration incorporates higher field water salinity during a sensitive growth stage, and lower field water salinity during less sensitive growth stages. Ideally, growth-stage specific salinity thresholds could be developed; however, this was not feasible in this experiment, as the salinity concentrations were not controlled.

Nevertheless, the approach taken to establish this threshold estimate addresses a key concern that many have with the traditional threshold-slope approach. Generally, salinity studies attempt to characterize the entire range of salinity stress, from 0 to 100% yield loss; therefore, they tend to have too few observations near the threshold value and too many above what is realistic in grower's fields. This tends to result in poor definition of the yield threshold (van Genuchten and Hoffman, 1984). For the previous  $1.9 \text{ dS m}^{-1}$  threshold, the 95% confidence interval was  $0.6\text{--}3.2 \text{ dS m}^{-1}$  (Grattan et al., 2002; Grieve et al., 2012). In this study, the 95% confidence interval for the  $0.88 \text{ dS m}^{-1}$  threshold was  $0.35\text{--}1.36 \text{ dS m}^{-1}$  (Fig. 5). The improved definition of this threshold estimate is likely due to this study having more observations near the expected threshold value. This, along with this study being done under commercial field conditions, with realistic seasonal variations in EC<sub>fw</sub>, makes this season-average threshold more applicable to commercial rice fields. Future work should be done to develop salinity thresholds at various growth stages, as this could not be achieved in this study.

#### 4.3. Spatio-temporal field water salinity dynamics

Quantifying the spatial and temporal variation of water salinity in rice fields is the first step towards developing potential management solutions to prevent salinity induced yield loss. Among all fields, consistent spatial water salinity patterns emerged: season-average EC<sub>fw</sub> was greater in C3 positions than in A1 positions by an average of 79% (Table 3). Additionally, in most field sites, the maximum EC<sub>fw</sub> occurred in the bottom basin, and ranged from  $0.36$  to  $6.06 \text{ dS m}^{-1}$  (Table 2). Similarly, Scardaci et al. (2002), Simmonds et al. (2013) and Shannon et al. (1998), all reported higher water salinity in bottom basins of rice fields. It is likely that EC<sub>fw</sub> increases with increasing distance from the irrigation inlet due to evapo-concentration of salts in the field water and the subsequent movement of that salt concentrated water down the field.

A consistent temporal water salinity pattern also emerged: relative EC<sub>fw</sub> is higher early in the season (Fig. 3, Fig. 6) and EC<sub>fw</sub> maxima generally occurred from week 2 to week 7 after planting (Table 2). This is similar to results reported by Scardaci et al. (2002). The rise in EC<sub>fw</sub> early in the season is likely due to two factors. First, low canopy cover during this period allows for high rates of evaporation from the water surface thereby concentrating salts in the field water. Second, it is common for growers to allow field water to subside early in the season for the application of foliar herbicides (University of California Cooperative Extension, 2015). As the field water subsides, the surface area to volume ratio of the field water increases such that evapo-concentration increases. In this study, low water depths during this period coincided with higher water salinity (Fig. 3).

#### 4.4. Modeling field water salinity

Consistent spatial trends of water salinity among fields allowed for the development of a model capable of predicting season-average water salinity throughout a rice field under zero-drainage (Fig. 6; Table 6). Position within a field, which is a combination of the longitudinal distance and lateral distance from the irrigation inlet, accounted for 82% of the explained variation in the model. This result indicates the importance that distance, and in effect

field size, has on water salinity build-up within flooded rice fields. For the same irrigation water and soil salinity, larger fields are at greater risk of having field water salinity increase to yield-reducing concentrations.

The other factor influencing water salinity build-up within a field was the preseason soil salinity. Soil salinity had a significant effect on water salinity build-up early in the season, contributed to 49% of the explained variance in the early-season model (Table 6). Furthermore, among all field sites, the higher EC<sub>fw</sub> maxima occurred in sites with high EC<sub>e</sub> (Table 2). These results may be explained by considering vertical water and solute movement in flooded rice fields. Rice fields in the region tend to have low rates of percolation during the growing season (Linquist et al., 2015). This, along with low transpiration rates early in the growing season results in low advective flow downward. Studies by Bachand et al. (2014a,b) show upward diffusion of solutes in flooded rice fields occurs during periods of minimal transpiration and that the rate of diffusion is dictated by concentration gradients. Therefore, it is likely that in fields with high soil salinity, salts were diffusing upward into the field water early in the growing season, contributing to greater observed field water salinity.

Temporal differences are also evident from these models. The early-season model had a substantially higher validation R<sup>2</sup>, 0.68, compared to the late-season model, 0.19 (Fig. 6). This is due to model parameters having less influence later in the growing season. Salts from the soil are less likely to diffuse upward later in the season when transpiration is high and there is high advective flow downward. Additionally, low evaporation later in the growing season, due to canopy cover, and a higher water depth, decreases the influence that the spatial position within a field (i.e. longitudinal and lateral distance) has on water salinity build-up within a field.

These models also allow comparisons to be made between zero-drainage and conventional-drainage fields. While the sample size for comparison was limited (only 3 fields under conventional-drainage), there is evidence suggesting tailwater drainage reduces field water salinity. During the early-season, water salinity in fields under conventional-drainage was overestimated (Fig. 6), indicating that tailwater drainage early in the season reduces field water salinity. This is similar to results reported by Scardaci et al. (2002). Tailwater drainage helps remove dissolved salts that accumulate in field water. The tailwater drainage early in the season, in fields under conventional-drainage, thus resulted in reduced water salinity in those fields.

These modeling results highlight the ability to sufficiently predict water salinity in rice fields with a few simple parameters. This study did not consider flow rates, slope of the field, or climatic effects. These factors could have an important contribution to explaining water salinity in a field and may have improved model estimates. However, it is shown, that with relatively few factors, field water salinity can be reasonably well predicted which facilitates application of these results for use by growers.

#### 4.5. Management implications

This study has several important implications for managing water to control salinity in rice fields. First, in fields with low soil and irrigation water salinity, practicing zero-drainage is a viable strategy to reduce water usage without harming yield. Seven of the eight field sites studied under zero-drainage, had low soil and irrigation water salinity, and in those sites, the field-average EC<sub>fw</sub> did not increase beyond the 0.88 dS m<sup>-1</sup> salinity threshold (Table 2). In the long-term however, zero-drainage may result in secondary soil salinization if amelioration efforts are not employed. One way to reduce the potential long-term soil salinity build-up is through winter flooding, a common practice in California to aid in rice straw decomposition (Linquist et al., 2006). Winter flooding can bring

up and export solutes that have built-up during the growing season (Bachand et al., 2014a). The degree to which winter flooding can reduce salt concentrations in rice fields under long-term zero-drainage management merits further investigation.

Second, in fields with either high soil or irrigation water salinity, maintaining a higher water depth and allowing for tailwater drainage early in the season will help reduce field water salinity. The highest field water salinity occurred early in the growing season (Table 2; Fig. 3) when rice is sensitive to salinity (Heenan et al., 1988; Fraga et al., 2010; Pearson and Bernstein 1959; Zeng et al., 2001). In these high salinity fields, salt flow from the soil to the field water and high rates of evapo-concentration, may increase field water salinity to yield-reducing concentrations. Increasing water depth during this period allows for dilution of dissolved salts. Additionally, allowing tailwater drainage during this period may also help reduce field water salinity (Fig. 6). These practices, however, may not be feasible with many pesticide regimes commonly employed in California, as contact herbicides require low water depth to ensure proper coverage, and water holding periods imposed after pesticide applications prevents tailwater drainage.

Lastly, in most fields studied, season-average field water salinity reached concentrations that were 50% greater than the irrigation water salinity (Fig. 6). Therefore, to avoid season-average field water salinity increasing beyond the 0.88 dS m<sup>-1</sup> threshold in the bottom of an average sized field (35 ha in this study), it is recommended to maintain irrigation water salinity below 0.6 dS m<sup>-1</sup>. This criterion for irrigation water salinity is similar to the 0.75 dS m<sup>-1</sup> reported by Finfrock et al. (1960). To maintain irrigation water salinity below 0.6 dS m<sup>-1</sup>, the use of groundwater as an irrigation source should be minimized, and irrigation districts should carefully portion the amount of high salinity recycled water allowed in the supplied surface water. Furthermore, as increases in water salinity within a field are largely a function of distance from the irrigation inlet, in areas with high soil or irrigation water salinity, smaller fields and multiple irrigation inlets should be considered.

#### Acknowledgements

We would like to thank the California Rice Research Board for providing funding for this study. Furthermore, we would like to thank the staff and students in the Agroecosystems laboratory at UC Davis, most especially Cesar Abrenilla, for their support and assistance throughout this project.

#### Appendix A. Supplementary data

Supplementary data associated with this article can be found, in the online version, at <https://doi.org/10.1016/j.agwat.2017.09.016>.

#### References

- Ayers, R.S., Westcot, D.W., 1985. *Water quality for agriculture*. FAO Irrig. Drain, Vol. 29. FAO, Rome.
- Bachand, P.A.M., Bachand, S.M., Fleck, J.A., Alpers, C.N., Stephenson, M., Windham-Myers, L., 2014a. *Methylmercury production in and export from agricultural wetlands in California: USA: the need to account for physical transport processes into and out of the root zone*. Sci. Total Environ. 472, 957–970.
- Bachand, P.A.M., Bachand, S.M., Fleck, J.A., Anderson, F., Windham-Myers, L., 2014b. *Differentiating transpiration from evaporation in seasonal agricultural wetland and the link to advective fluxes in the root zone*. Sci. Total Environ. 484, 232–248.
- Bartoń, K., 2016. MuMln: Multi-Model Inference. <https://CRAN.R-project.org/package=MuMln>.
- Bates, D., Maechler, M., Bolker, B., Walker, S., 2016. Lme4: Linear Mixed-Effects Models Using Eigen and S4. <https://CRAN.R-project.org/package=lme4>.
- Bazihizina, N., Barrett-Lennard, E.G., Colmer, T.D., 2012. *Plant growth and physiology under heterogeneous salinity*. Plant Soil 354, 1–19.
- Becker, R.A., Wilks, A.R., Brownrigg, R., Minka, T.P., Deckmyn, A., 2016. Maps: Draw Geographical Maps. <https://CRAN.R-project.org/package=maps>.

- Bivand, R., Lewin-Koh, N., 2016. Maptools: Tools for Reading and Handling Spatial Objects. <https://CRAN.R-project.org/package=maptools>.
- Bouman, B.A.M., Humphreys, E., Tuong, T.P., Barker, R., 2007. Rice Water Adv. Agron. 92, 187–237.
- Burnham, K.P., Anderson, D.R., 2002. <EDN></EDN>. In: Model Selection and Multimodel Inference: A Practical Information-theoretic Approach, 2nd edition. Springer-Verlag, New York.
- Burt, R., 2014. Soil Survey Laboratory Methods Manual. SSIR No. 42. Government Printing Office, Washington, DC: U.S. (Version 5.0. NRCS-USDA).
- CIMIS, 2016. California Irrigation Management Information System (Internet Resource) <http://www.cimis.water.ca.gov/WSNReportCriteria.aspx>.
- Castillo, E.G., Tuong, T.P., Ismail, A.M., Inubushi, K., 2007. Response to salinity in rice: comparative effects of osmotic and ionic stresses. Plant Prod. Sci. 10, 159–170.
- Connor, J.D., Schwabe, K., King, D., Knapp, K., 2012. Irrigated agriculture and climate change: the influence of water supply variability and salinity on adaptation. Ecol. Econ. 77, 149–157.
- Dickey, J., Nuss, C., 2002. Salinity distribution and impact in the sacramento valley. USCID Water Management Conference on Helping Irrigating Agriculture Adjust to TMDLs.
- Ehrler, W., 1960. Some effects of salinity on rice. Bot. Gaz. 122, 102–104.
- Finfrock, D.C., Raney, F.C., Miller, M.D., Booher, L.J., 1960. Water management in rice production. In: Division of Agricultural Sciences. University of California, pp. 131 (Leaf).
- Fraga, T.I., Carmona, F.C., Anghinomi, I., Junior, S.A.G., Marcolin, E., 2010. Flooded rice yield as affected by levels of water salinity in different stages of its cycle. R. Bras. Ci Solo 34, 175–182.
- Fraiture, C.D., Wichelns, D., 2010. Satisfying future water demands for agriculture. Agric. Water Manage. 97, 502–511.
- Grattan, S.R., Zeng, L., Shannon, M.C., Roberts, S.R., 2002. Rice is more sensitive to salinity than previously thought. Calif. Agric. 56, 189–198.
- Grattan, S.R., 2002. Irrigation Water Salinity and Crop Production. Water Quality Fact Sheet. Division of Agriculture and Natural Resources. University of California, UC DANR electronic publication no. 8066, Oakland, CA.
- Grieve, C.M., Grattan, S.R., Maas, E.V., 2012. Plant salt tolerance. In: Wallender, W.W., Tanji, K.K. (Eds.), ASCE Manual and Reports on Engineering Practice No. 71 Agricultural Salinity Assessment and Management, 2nd edition. ASCE, Reston, VA, pp. 405–459 (Chapter 13).
- Groemping, U., Matthias, L., 2013. h. In: Relaimpo: Relative Importance of Regressors in Linear Models. <https://CRAN.R-project.org/package=relaimpo>.
- Hanak, E., Lund, J.R., 2012. Adapting California's water management to climate change. Clim. Change 111, 17–44.
- Heenan, D.P., Lewin, L.G., McCaffery, D.W., 1988. Salinity tolerance in rice varieties at different growth stages. Aust. J. Exp. Agric. 28, 343–349.
- Hijmans, R.J., 2015. Raster: Geographic Data Analysis and Modeling. <https://CRAN.R-project.org/package=raster>.
- Hill, J.E., Scardaci, S.C., Roberts, S.R., Tiedeman, J., Williams, J.F., 1991. Rice irrigation systems for tailwater management. Univ. Calif. Div. Ag. Nat. Res. Pub. 21490.
- Hill, J.E., Williams, J.F., Mutters, R.G., Greer, C.A., 2006. The California rice cropping system: agronomic and natural resource issues for long-term sustainability. Paddy Water Environ. 4, 13–19.
- Homae, M., Schmidhalter, U., 2008. Water integration by plants root under non-uniform soil salinity. Irrig. Sci. 27, 83–95.
- Howitt, R.E., MacEwan, D., Medellín-Azuara, J., Lund, J.R., Sumner, D.A., 2015. Economic Analysis of the 2015 Drought for California Agriculture. Center for Watershed Sciences, UC, Davis, Davis, CA.
- Kijne, J.W., 2006. Abiotic stress and water scarcity: identifying and resolving conflicts from plant level to global level. Field Crop Res. 97, 3–18.
- Kuhn, M., 2016. Caret: Classification and Regression Training. <https://cran.r-project.org/package=caret>.
- Kuznetsova, A., Brockhoff, P.B., Christensen, R.H.B., 2016. LmerTest: Tests in Linear Mixed Effects Models. <https://cran.r-project.org/package=LmerTest>.
- Läuchli, A., Grattan, S.R., 2007. Plant growth and development under salinity stress. In: Jenks, M.A., Hasegawa, P.M., Mohan, J.S. (Eds.), Advances in Molecular Breeding Towards Drought and Salt Tolerant Crops. Springer, Berlin, pp. 1–32.
- Lekakis, E., Aschonitis, V., Pavlata-Ve, A., Papadopoulos, A., Antonopoulos, V., 2015. Analysis of temporal variation of soil salinity during the growing season in a flooded rice field of thessaloniki plain-Greece. Agron. J. 5, 35–54.
- Lindeman, R.H., Merenda, P.F., Gold, R.Z., 1980. Introduction to Bivariate and Multivariate Analysis. Scott Foresman, Glenview, IL.
- Linquist, B.A., Brouder, S.M., Hill, J.E., 2006. Winter straw and water management effects on soil nitrogen dynamics in California rice systems. Agron. J. 98, 1050–1059.
- Linquist, B.A., Snyder, R., Anderson, F., Espino, L., Inglese, G., Marras, S., Moratiel, R., Mutters, R.G., Niccolosi, P., Rejmanek, H., Russo, A., Shapland, T., Song, Z., Swelam, A., Tindula, G., Hill, J.E., 2015. Water balances and evapotranspiration in water- and dry-seeded rice systems. Irrig. Sci. 33, 375–385.
- Maas, E.V., Grattan, S.R., 1999. Crop yields as affected by salinity. In: Skaggs, R.W., van Schilfgaarde, J. (Eds.), Agricultural Drainage. Madison. ASA-CSSA-SSSA, WI, pp. 55–108.
- Maas, E.V., Hoffman, G.J., 1977. Crop salt tolerance—current assessment. J. Irrig. Drain. Eng. 103, 115–134.
- Mirchi, A., Madani, K., Roos, M., Watkins, D.W., 2013. Climate change impacts on California's water resources. In: Schwabe, K., et al. (Eds.), Drought in Arid and Semi-Arid Regions, pp. 301–322 (Chapter 17).
- Molden, D., Oweis, T., Steduto, P., Bindraban, P., Hanjra, M.A., Kijne, J., 2010. Improving agricultural water productivity: between optimism and caution. Agric. Water. Manage. 97, 528–535.
- Morita, S., Yamazaki, K., 1993. Root system. In: Matsuo, T., Hoshikawa, K. (Eds.), Science of the Rice Plant, Vol. 1. Morphology. Food and Agriculture Policy Research Center, Tokyo, pp. 161–186.
- Munns, R., Tester, M., 2008. Mechanisms of salinity tolerance. Annu. Rev. Plant Biol. 59, 651–681.
- Nakagawa, S., Schielzeth, H., 2013. A general and simple method for obtaining R2 from Generalized Linear Mixed-effects Models. Methods Ecol. Evol. 4, 133–142.
- Narale, R.P., Subramanyam, T.K., Mukherjee, R.K., 1969. Influence of salinity on germination, vegetative growth, and grain yield of rice (*Oryza sativa* var. Dular). Agron. J. 61, 311–344.
- Pearson, G.A., Bernstein, L., 1959. Salinity effects at several growth stages of rice. Agron. J. 51, 654–658.
- Pearson, G.A., 1959. Factors influencing salinity of submerged soils and growth of Caloro rice. Soil Sci. 37, 198–206.
- Pike, A.C., Mueller, T.G., Schörgendorfer, A., Shearer, S.A., Karathanasis, A.D., 2009. Erosion index derived from terrain attributes using logistic regression and neural networks. Agron. J. 101, 1068–1079.
- R Core Team, 2015. R: A Language and Environment for Statistical Computing. R Foundation for Statistical Computing, Vienna, Austria <https://www.R-project.org/>.
- Scardaci, S.C., Eke, A.U., Hill, J.E., Shannon, M.C., Rhoades, J.D., 1996. Water and soil salinity studies on California rice. In: Rice. University of California Cooperative Extension (Publication No. 2).
- Scardaci, S.C., Shannon, M.C., Grattan, S.R., Eke, A.U., Roberts, S.R., Goldman-Smith, S., Hill, J.E., 2002. Water management practices can affect salinity in rice fields. Calif. Agric. 56, 184–188.
- Schewe, J., Heinke, J., Gerten, D., Haddeland, I., Arnell, N.W., Clark, D.B., Dankers, R., Eisner, S., Fekete, B.M., Colon-Gonzalez, F.J., Gosling, S.N., Kim, H., Liu, X., Masaki, Y., Portmann, F.T., Satoh, Y., Stacke, T., Tang, Q., Wada, Y., Wisser, D., Albrecht, T., Frieler, K., Piontek, F., Warszawski, L., Kabat, P., 2014. Multimodal assessment of water scarcity under climate change. PNAS 111, 3245–3250.
- Scudiero, E., Skaggs, T.H., Corwin, D.L., 2015. Regional-scale soil salinity assessment using Landsat ETM + canopy reflectance. Remote Sens. Environ. 169, 335–343.
- Shalhevet, J., 1994. Using water of marginal quality for crop production: major issues. Agric. Water Manage. 25, 233–269.
- Shannon, M.C., Rhoades, J.D., Draper, J.H., Scardaci, S.C., Spyres, M.D., 1998. Assessment of salt tolerance in rice cultivars in response to salinity problems in California. Crop Sci. 38, 394–398.
- Simmonds, M.B., Plant, R.E., Peña-Barragán, J.M., Van Kessel, C., Hill, J.E., Linquist, B.A., 2013. Underlying causes of yield spatial variability and potential for precision management in rice systems. Precis. Agric. 14, 512–540.
- Stevens, A., Miralles, I., Van Wesemael, B., 2012. Soil organic carbon predictions by airborne imaging spectroscopy: comparing cross-Validation and validation. Soil Sci. Soc. Am. J. 76, 2174–2183.
- USDA, 2013. Farm and Ranch Irrigation Survey (FRIS) (Table 36).
- University of California Cooperative Extension, 2015. California Rice Production Workshop Manual.
- Venkateswarlu, J., Ramesam, M., Mohan, Murali, Rao, G.V., 1972. Salt tolerance in rice varieties. J. Ind. Soc. Soil Sci. 20, 169–213.
- Wallace, J.S., 2000. Increasing agricultural water use efficiency to meet future food production. Agric. Ecosyst. Environ. 82, 105–119.
- Wickham, H., Chang, W., 2016. Ggplot2: An Implementation of the Grammar of Graphics. <https://cran.r-project.org/package=ggplot2>.
- Wickham, H., 2016. Gtable: Arrange 'Grobs' in Tables. <https://cran.r-project.org/package=gtable>.
- Yoshida, S., 1981. Fundamental of Rice Crop Science. IRRI, Los Baños Philippines.
- Zeng, L., Shannon, M.C., Lesch, S.M., 2001. Timing of salinity stress affects rice growth and yield components. Agric. Water Manage. 48, 191–206.
- van Genuchten, M.Th., Hoffman, G.J., 1984. Analysis of crop salt tolerance data. In: Shainberg, I., Shalhevet, J. (Eds.), Soil Salinity Under Irrigation, Processes and Management: Ecological Studies 51. Springer-Verlag, New York, pp. 258–271.